
SONG: SELF-ORGANIZING NEURAL GRAPHS

A PREPRINT

Łukasz Struski

Faculty of Mathematics and Computer Science
Jagiellonian University
Kraków, Poland
lukasz.struski@uj.edu.pl

Tomasz Danel

Faculty of Mathematics and Computer Science
Jagiellonian University
Kraków, Poland
tomasz.danel@ii.uj.edu.pl

Marek Śmieja

Faculty of Mathematics and Computer Science
Jagiellonian University
Kraków, Poland
marek.smieja@uj.edu.pl

Jacek Tabor

Faculty of Mathematics and Computer Science
Jagiellonian University
Kraków, Poland
jacek.tabor@uj.edu.pl

Bartosz Zieliński

Faculty of Mathematics and Computer Science
Jagiellonian University
Kraków, Poland
bartosz.zielinski@uj.edu.pl

ABSTRACT

Recent years have seen a surge in research on deep interpretable neural networks with decision trees as one of the most commonly incorporated tools. There are at least three advantages of using decision trees over logistic regression classification models: they are easy to interpret since they are based on binary decisions, they can make decisions faster, and they provide a hierarchy of classes. However, one of the well-known drawbacks of decision trees, as compared to decision graphs, is that decision trees cannot reuse the decision nodes. Nevertheless, decision graphs were not commonly used in deep learning due to the lack of efficient gradient-based training techniques. In this paper, we fill this gap and provide a general paradigm based on Markov processes, which allows for efficient training of the special type of decision graphs, which we call Self-Organizing Neural Graphs (SONG). We provide an extensive theoretical study of SONG, complemented by experiments conducted on Letter, Connect4, MNIST, CIFAR, and TinyImageNet datasets, showing that our method performs on par or better than existing decision models.

1 Introduction

Neural networks (NNs) and decision trees (DTs) are two exceptionally powerful machine learning models with a rich and successful history in machine learning. They typically come with mutually exclusive benefits and limitations. NNs outperform conventional pipelines by jointly learning to represent and classify data [15]. However, they are widely opaque and suffer from a lack of transparency and explainability [30]. On the other hand, it is easy to explain a prediction of DTs because it depends on a relatively short sequence of decisions. However, they usually do not generalize as well as deep neural networks [8]. As a result, a strong focus is recently put on joining the positive aspects of both models [2, 8, 13, 23, 24, 34, 36, 38]. There are methods that combine NNs and soft decision trees with partial membership in each node [8, 13, 24, 34]. Others use trees to explain NNs [5, 39] or to obtain their optimal hierarchical structure [2, 23, 36]. Finally, some models replace the final softmax layer of a neural network with a hierarchical binary decision tree [20, 21, 38].

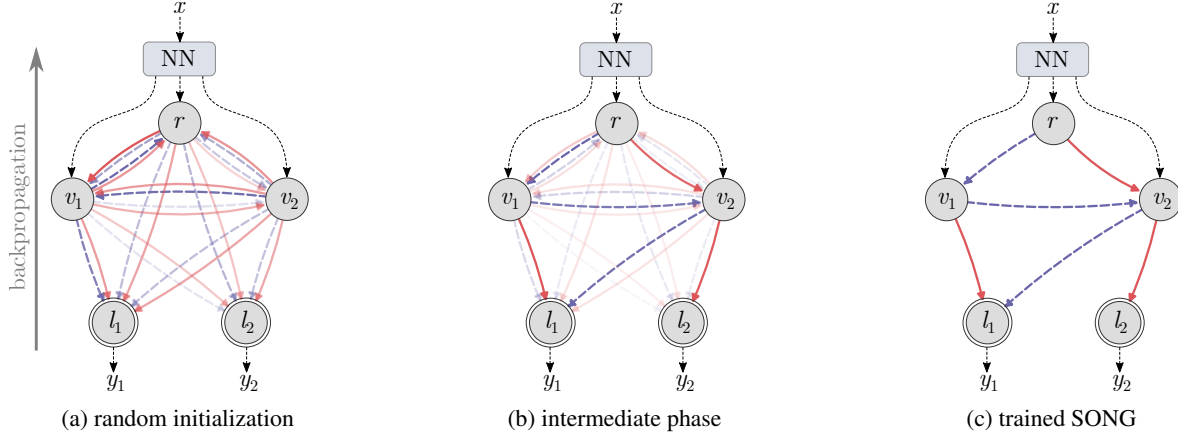


Figure 1: Training stages of SONG that uses gradient descent to modify the graph structure and transition probabilities. The input x can be transformed by a neural network (NN) which extracts a vector representation. After random initialization, the graph with root r , nodes v_1 and v_2 , and leaves l_1 and l_2 has a structure of a weak clique (a). In the successive stages of the training, the entropy of edge weights grows (b), resulting in a sparse binary graph, with exactly two edges outgoing from each node (c). Notice that SONG contains two alternative sets of edges between the nodes (dashed blue arrows and solid red arrows, respectively) that are combined based on the input (see Section 3 for details).

While decision trees can increase the performance and interpretability of NNs, they usually suffer from exponential growth with depth [32], repeating nodes [8], and suboptimal structure, often selected manually before training [38]. Hence, more and more attention is put on combining NNs with decision graphs instead of trees [4, 9, 11, 22, 37]. Decision graphs have a few advantages when compared to decision trees. They have a flexible structure that allows multiple paths from the root to each leaf. As a result, nodes are reused, which solves the replication problem [26]. Moreover, they require substantially less memory while considerably improving generalization [33]. Nevertheless, decision graphs are not used commonly in deep learning due to a lack of efficient gradient-based training techniques.

In this paper, we introduce Self-Organizing Neural Graphs (SONGs)¹, a special type of decision graphs with two alternative sets of edges between the nodes (represented by two colors in Figure 1) that are combined depending on the input. SONG generalizes methods like Soft Decision Tree (SDT) [8] and Neural-Backed Decision Trees (NBDT) [38] and as a differentiable solution is applicable to any deep learning pipeline (Figure 1). Moreover, SONG can strengthen or weaken an edge between any pair of nodes during training to optimize its structure. In contrast, the existing methods have a fixed structure of binary tree [8, 38], with a specified set of edges that cannot change during training. We illustrate the process of determining the optimal structure by SONG in Figure 1. At the beginning, the edges have random weights. However, in successive steps of training, the structure is corrected with backpropagation. As a result, it gets sparse and converges to the binary directed acyclic graphs [28] (see Figure 1c). We prove this statement in Section 4.

Our contributions can be summarized as follows:

- We introduce Self-Organizing Neural Graphs (SONGs), a new paradigm of end-to-end decision graph training based on Markov processes that simultaneously learn the optimal graph structure and transition probabilities.
- Our model is fully differentiable and thus suitable for combined training with other deep learning models.
- We prove empirically and theoretically that SONGs during training converge to sparse binary acyclic graphs and can be interpreted as diagrams of consecutive decisions.
- Our method performs on par or outperforms decision trees trained in a similar setup and does not require the graph/tree structure to be predefined before training.

2 Related works

Decision trees Numerous Decision Tree (DT) algorithms have been developed over the years [18, 19, 29, 31] and after the success of deep learning, much research relates to combining DTs with neural networks. As a result, Soft Decision Tree (SDT) was introduced, allowing for the partial membership of a sample in the nodes that make up the tree structure [34], also trained in distillation setup [8]. This idea was also used in [13] that trains a set of classification

¹The code is available at: [anonymized]

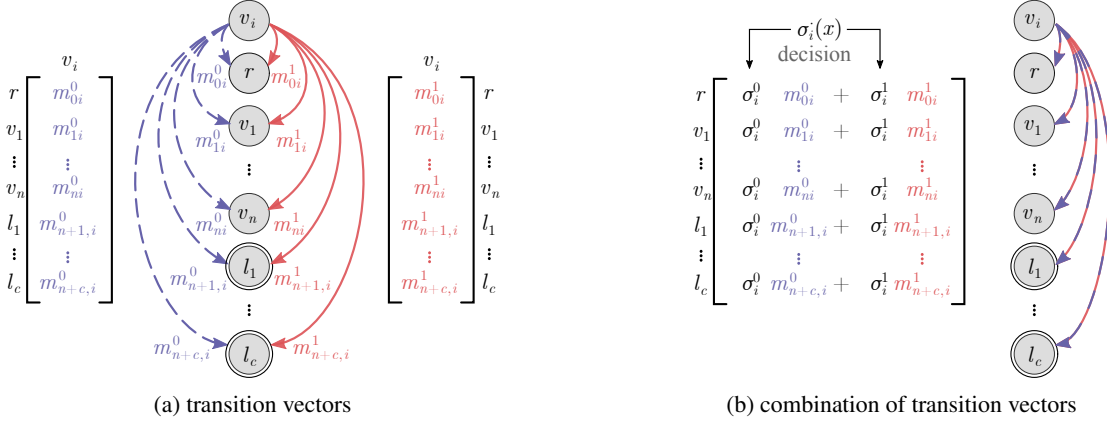


Figure 2: SBDG contains two alternative transition vectors $m_{\cdot i}^0$ and $m_{\cdot i}^1$ that aggregate the probability of moving from a particular node v_i to all other nodes. In (a), they are represented as dashed blue and solid red arrows, respectively. Each node obtains input data x and makes a binary decision with probabilities σ_i^0 and σ_i^1 of using one transition or another. As $\sigma_i^0 + \sigma_i^1 = 1$, SBDG can be transformed to a standard directed graph by combining $m_{\cdot i}^0$ and $m_{\cdot i}^1$, as presented in (b).

trees and a backbone network in an end-to-end manner. Moreover, it was recently used in [24] to faithfully visualize the model using nodes with prototypes [6] instead of classifiers. Trees were also used to explain the previously trained black box models [5, 39]. More advanced methods automatically generate deep networks with a tree structure in a multi-step or an end-to-end manner [1, 2, 23, 36, 38]. In contrast to the presented methods, our approach has a structure of a graph trained together with other model parameters in an end-to-end manner.

Decision graphs A decision graph is a well-studied classifier and has been used to solve many real-world problems [35]. When implemented as Directed Acyclic Graphs (DAG), it leads to accurate predictions while having lower model complexity, subtree replication, and training data fragmentation compared to decision trees [33]. However, most of the existing algorithms for learning DAGs involve training a conventional tree that is later manipulated into a DAG [7, 12, 25, 27] and, as such, are difficult to be directly adopted into neural networks. Hence, alternative approaches were proposed, like [4], which maintains the structure of the standard convolutional neural networks (CNNs) but uses additional routing losses at each layer to maximize the class-wise purity (like in growing decision trees) using data activation according to the class label distribution. Another method [37] introduces identity skip-connections similar to ResNets [9] that are executed or skipped depending on the gate response for an input. A similar gate mechanism was used in [22] to choose branches specialized for different inputs, whose outputs are combined to make the final predictions. Finally, [11] embeds infinitely many filters into low dimensional manifolds parameterized by compact B-splines and maximizes the mutual information between spline positions and class labels to specialize for classification tasks optimally. Such a mechanism significantly reduces runtime complexity. In contrast to existing methods, SONG is a directed graph that can be adapted to any deep architecture and trained in an efficient gradient-based manner.

3 Self-organizing neural graphs

Self-Organizing Neural Graphs (SONGs) are a special type of decision graphs with two alternative sets of edges between the nodes. To better explain the method, we first define the abstract structure of this special type of graph that we call Soft Binary Directed Graph (SBDG), and then we define SONG as the implementation of this abstract structure. SBDG is considered binary because there are two alternative sets of edges, and soft because those sets are combined depending on the input, resulting in one target set of edges. In the remaining part of the section, we describe how to use SONGs as a decision model, present method limitations, and show how to overcome them with additional regularizers. The below definitions correspond to single-label classification for the clarity of description. However, they could be easily extended to other tasks, like multi-label classification or regression.

Soft binary directed graphs Soft Binary Directed Graph (SBDG) is a directed graph, which can be viewed as a probabilistic model. It is defined as graph $G = (V, E^0, E^1)$, with V corresponding to a set of nodes and E^0, E^1 corresponding to two alternative sets of edges, where:

- Set V contains two types of nodes:
 - internal nodes v_0, \dots, v_n , with v_0 specified as root r ,

- leaves l_1, \dots, l_c , each exclusively associated with one class from set $\{1, \dots, c\}$,
- Set E^d , for $d \in \{0, 1\}$, contains all possible edges with weights m_{ji}^d corresponding to the probability of moving from node $u_i \in V$, as presented in Figure 2a. In the following, the aggregated probabilities of moving from node u_i to other nodes will be called a transition vector and denoted as $m_{\cdot i}^d$.
- If u_i is a leaf, then $m_{ji}^d = \delta_{ji}$ (Kronecker delta), which means that it is impossible to move out from the leaves.
- Each internal node u_i makes binary decisions $d \in \{0, 1\}$ with probabilities σ_i^d of using edges from set E^d .
- As $\sigma_i^0 + \sigma_i^1 = 1$, G can be transformed to a standard directed graph by combining $m_{\cdot i}^0$ and $m_{\cdot i}^1$ using the following formula for each node u_i : $\sigma_i^0 m_{\cdot i}^0 + \sigma_i^1 m_{\cdot i}^1$. This process is presented in Figure 2b.

Notice that if all transition vectors are binary, then after removing the edges with zero probability, SBDG becomes a binary directed graphs [28].

Self-organizing neural graphs Self-Organizing Neural Graph (SONG) is a fully differentiable adaptation of SBDG that can be combined with various deep architectures. Assuming that $x \in X$ is the input sample, SONG is defined as $\mathcal{G} = (\mathcal{V}, \mathcal{E}^0, \mathcal{E}^1)$, where $\mathcal{V}, \mathcal{E}^0, \mathcal{E}^1$ implement V, E^0 , and E^1 of SBDG, and are obtained in the following way:

- The probability of decision $d = 1$ in node u_i is obtained as $\sigma_i^1(x) = \sigma(xw_i + b_i)$, where σ is the sigmoid logistic function, w_i is a filter function, and b_i is a bias².
- The probability of decision $d = 0$ equals $\sigma_i^0(x) = 1 - \sigma_i^1(x)$.
- The probability of moving from internal nodes is defined by two matrices $M^d = [m_{ji}^d] \in \mathbb{R}^{(n+c) \times n}$, for $d = \{0, 1\}$, with positive values and columns summing up to 1.

Notice that $\{w_i\}_{i=1, \dots, n}$, $\{b_i\}_{i=1, \dots, n}$, M^0 , and M^1 are trainable parameters of the model. Moreover, we define a directed graph $\mathcal{G}_x = (\mathcal{V}, \mathcal{E})$ generated for input x where \mathcal{E} corresponds to the combination of matrices M^0 and M^1 :

$$M_x = \mathbb{1}\sigma_x^T \odot M^1 + \mathbb{1}(\mathbb{1} - \sigma_x)^T \odot M^0, \quad (1)$$

where $\sigma_x = [\sigma_1^1(x), \dots, \sigma_n^1(x)]^T$, symbol \odot denotes the Hadamard product, and $\mathbb{1}$ is the all-ones vector of dimension n (see Figure 3).

Decision model Matrix M_x contains the probability of moving from internal nodes to all nodes of the graph. However, to apply the theory of the Markov processes, it needs to be extended by columns corresponding to the leaves (as presented on the left side of Figure 3):

$$P_x = \begin{bmatrix} M_x & \begin{smallmatrix} 0 \\ \vdots \\ 0 \end{smallmatrix} \\ \begin{smallmatrix} \vdots \\ \vdots \\ \vdots \end{smallmatrix} & \mathbb{I} \end{bmatrix} \in \mathbb{R}^{(n+c) \times (n+c)}, \quad (2)$$

where $0 \in \mathbb{R}^{n \times c}$ is zero matrix, $\mathbb{I} \in \mathbb{R}^{c \times c}$ is an identity matrix. As a result, we obtain a square stochastic (transition) matrix used to describe the transitions of a Markov chain. While P_x contains the probability of moving from u_i to u_j in one time step, it can be easily used to obtain a similar probability for N steps by calculating the N -th power of P_x . Finally, the resulting matrix can be multiplied by vector $v = [1, 0, \dots, 0]^T$ to obtain the probability of moving from the root to any node of the graph, including leaves, whose probability is the output of the model. We present a simple example illustrating this process on the right side of Figure 3. More examples are provided in Supplementary Materials.

Regularizations Similarly as in Soft Decision Trees (SDT) [8], we observe that our graphs require additional training regularizers. The reasons for that are threefold. First, SONG may get stuck on plateaus in which one or more $\sigma_i^d(x)$ is 0 for all input samples x , and the gradient of the sigmoid logistic function for this decision is always very close to zero. Second, if SONG is uncertain of its predictions, it can safely hold the probabilities in internal nodes instead of moving them to leaves, which results in a small accumulated probability in the latter. Third, SONG tends to binarize what is positive in general, but if this binarization appears too early, the model can get stuck in a local minimum. Therefore, to prevent model degeneration, we introduce three types of regularization. The first one, called node regularization, is based on [8] and encourages each internal node to make equal use of both sets of edges \mathcal{E}^0 and \mathcal{E}^1 . The second one, called leaves regularization, enforces the summary probabilities in leaves to be close to 1. Finally, we use Gumbel-softmax [10] with a fixed temperature to better explore the trajectories of the graph. Details are provided in Supplementary Materials.

4 Theoretical analysis

In this section, we prove that for a perfectly trained SONG (with cross-entropy or binary cross-entropy loss equals 0), it has no cycles and converges to a binary directed acyclic graph.

²In practice, this probability could also be obtained with any NN that ends with a sigmoid function.

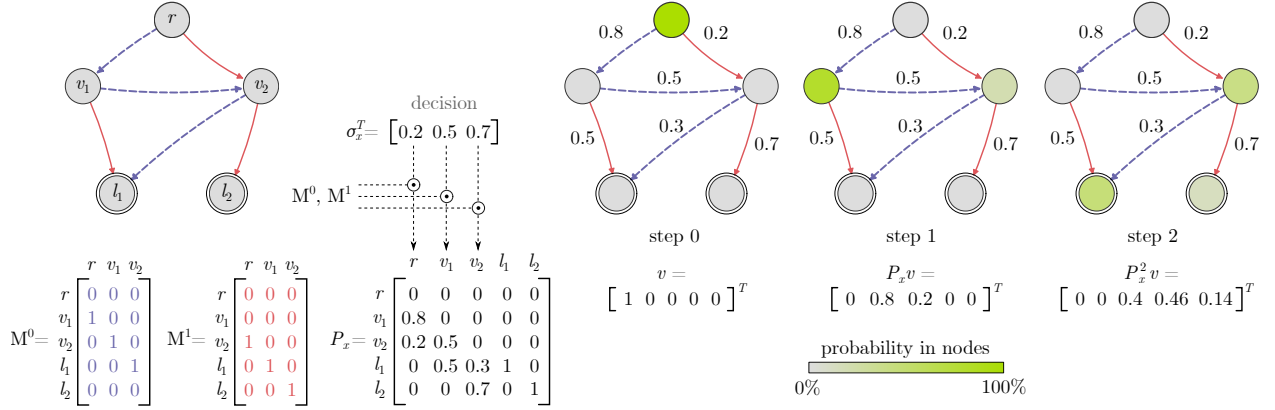


Figure 3: Construction of the transition matrix and successive steps of our Markov process. On the left, a graph with its matrices M^0 and M^1 is presented, followed by an exemplary decision vector σ_x and the resulting matrix P_x . On the right, the flow in a graph is depicted for 3 consecutive steps. At first, the probability is entirely placed in the root. In the next steps, the distribution splits between nodes according to the transition probabilities, reaching leaves in step 3. The probabilities in the leaves after all steps are class probabilities inferred by the model (the number of steps is considered as a method hyperparameter).

In our theoretical results, we consider SONG as the probabilistic model over trajectories. A trajectory of length N , starting at the root of SBDG G , is defined as $T = (u_{i_t})_{t=1..N}$ with binary decision $d_t \in \{0, 1\}$, $i_t \in I$, where I denotes the set of node indexes. Thus, our trajectory starts at the root ($i_0 = 0$) and successively passes through nodes $u_{i_{t_1}}, \dots, u_{i_{t_N}}$. The position of trajectory after time t is defined as $T(t) = u_{i_t}$ and the probability of trajectory T is defined as

$$\text{prob}(T; G) = \prod_{t=1}^N (\sigma_{i_{t-1}}^{d_t} \cdot m_{i_{t-1}i_t}^{d_t}).$$

Then the probability of reaching leaf l after N steps with a random trajectory T equals $\text{prob}(T(N) = l | T \sim G)$, where $T \sim G$ denotes that we sample trajectories with respect to distribution given by $\text{prob}(\cdot; G)$.

Next, we introduce a binarized graph G , where we binarize the connections from any pair of nodes. For a fixed $d \in \{0, 1\}$, we denote $G[i, j; d]$ as the graph that makes a decision of moving from u_i to u_j with probability 1. In the following theorem, we show that if G has no cycles, then we can decompose the probability of its trajectory into the mixture of such binarized graphs.

Theorem 4.1. *Let G be a SBDG where the probability of visiting twice an arbitrary node by a trajectory of length N is zero. Moreover, u_i be an internal node, fixed $d \in \{0, 1\}$, and an arbitrary trajectory T of length N . Then*

$$\text{prob}(T; G) = \sum_{j=1}^n m_{ji}^d \text{prob}(T; G[i, j, d]). \quad (3)$$

Proof. Let $T = (u_{i_t})_{t=1..N}$ be a given trajectory and let us consider three cases of passing through node u_i . First case assumes that T does not pass through u_i , i.e. $i \neq i_t$ for $t = 1, \dots, N$. Then, directly from the definition of the trajectory's probability

$$\text{prob}(T; G) = \text{prob}(T; G[i, j, d]), \text{ for an arbitrary } j.$$

This completes the proof of (3) in this case. Hence, let us now consider the cases where the trajectory T passes through node u_i .

Suppose the second case, when T passes through u_i more than once. In this case, we will show that both the left and right sides of (3) are zero. Obviously, $\text{prob}(T; G) = 0$ follows directly from the assumption that the probability of visiting twice an arbitrary node by a trajectory of length N in G is zero. Assume, for an indirect proof that there exist j such that $m_{ji}^d \text{prob}(T; G[i, j, d]) > 0$. Then $m_{ji}^d > 0$, and if T passes through u_i and makes a decision d , then it has to move to u_j . Then

$$\text{prob}(T; G) = m_{ji}^d \text{prob}(T; G[i, j, d]) > 0$$

is a contradiction.

Let us consider the remaining, third case, when T passes through u_i only once, and makes a decision d . In other words, there exists a unique t such that $i_t = i$ and $d_t = d$. Observe that if $j = i_{t+1}$ then we move from u_i to

u_j and all the probabilities $\mathbf{prob}(T; G[i, l, d]) = 0$, for $l \neq j$. Moreover, since T visits u_i only once, we get $\mathbf{prob}(T; G) = m_{ji}^d \mathbf{prob}(T; G[i, j, d])$, which completes the proof. \square

We now show the consequences of the above theorem for the SONG model. For this purpose, we assume that $X = (x_i)_{i=1..K}$ where each x_i is associated with a label y_i . We also consider SONG \mathcal{G} trained on X for trajectories of length N . Thus for each pair (x, y) , we define the probability that a random trajectory of length N reaches leaf corresponding to y as $\mathbf{prob}(T(N) = y | T \sim \mathcal{G}_x)$. Then the accuracy of \mathcal{G} over set X is defined as the probability of predicting the correct class

$$\text{acc}(\mathcal{G}; X) = \frac{1}{K} \sum_{i=1}^K \mathbf{prob}(T(N) = y_i | T \sim \mathcal{G}_{x_i}).$$

As a direct consequence of Theorem 4.1, we formulate the following fact.

Theorem 4.2. *Let \mathcal{G}_x be SONG generated for $x \in X$ with no trajectory of length N that visits twice the same point with nonzero probability. Moreover, a node index $i \in \{1, \dots, n\}$ and $d \in \{0, 1\}$ are fixed. Then*

$$\text{acc}(\mathcal{G}; X) = \sum_{j=1}^n m_{ji}^d \text{acc}(\mathcal{G}[i, j, d]; X).$$

Proof. By Theorem 4.1, for an arbitrary point $x \in X$ (with class y) and trajectory of length N , we have

$$\mathbf{prob}(T; \mathcal{G}_x) = \sum_{j=1}^n m_{ji}^d \mathbf{prob}(T; \mathcal{G}_x[i, j, d]).$$

In consequence,

$$\mathbf{prob}(T(N) = y | T \sim \mathcal{G}_x) = \sum_{j=1}^n m_{ji}^d \mathbf{prob}(T(N) = y | T \sim \mathcal{G}_x[i, j, d]).$$

Averaging the above probability over all points from X and applying the definition of accuracy, we obtain the assertion of the theorem. \square

Observe that the above theorem implies that if we discretize connections in the graph by applying formula (4), then we do not decrease the accuracy of the model (statistically, we increase it):

Corollary 4.1. *Let \mathcal{G}_x be SONG generated for $x \in X$ with no trajectory of length N that visits twice the same point with nonzero probability. Moreover, let node index $i \in I$ and $d \in \{0, 1\}$ be fixed, and*

$$j = \arg \max_{\tilde{j}} \text{acc}(\mathcal{G}[i, \tilde{j}, d]; X). \quad (4)$$

Then

$$\text{acc}(\mathcal{G}; X) \leq \text{acc}(\mathcal{G}[i, j, d]; X).$$

We show that for a perfectly trained SONG (with CE or BCE loss equals 0), the assumptions of the above corollary hold.

Proposition 4.1. *Let us consider SONG classifier with N moves and x being a data point with class y , such that $\text{loss}(\mathbf{prob}(T(N) = y | T \sim \mathcal{G}_x), y) = 0$.*

Then no trajectory of length N in \mathcal{G}_x visits the same internal node twice with nonzero probability.

Proof. First observe, that directly from the fact that both CE and BCE are non-negative, $\text{loss}(\mathbf{prob}(T(N) = y | T \sim \mathcal{G}_x), y) = 0$ iff

$$\mathbf{prob}(T(N) = y | T \sim \mathcal{G}_x) = 1.$$

Now suppose that there exists a trajectory T with nonzero probability, which goes through a given internal node u twice, i.e. $T(t_1) = T(t_2) = v$ for $t_1 < t_2$. Observe that $T(t)$ is not a leaf for $t \in [t_1, t_2]$, since after reaching the leaf, we stay in it. Consider the trajectory \tilde{T} given by

$$\tilde{T}(t) = \begin{cases} T(t) & \text{for } t \leq t_1, \\ T(t_1 + s) & \text{for } t = t_1 + l(t_2 - t_1) + s, l \in \mathbb{N}, s \in \{0, \dots, t_2 - t_1\}. \end{cases}$$

In other words, this is a trajectory that forms a cycle after reaching u . Thus we does not end in a leaf with nonzero probability, which leads to a contradiction. \square

Table 1: Comparison of models with deep architecture in terms of model features and accuracy on MNIST, CIFAR10 (CIF10), CIFAR100 (CIF100), and TinyImageNet (TinyIN). ResNet18 was used for most models to extract the vector representation of input images, except for DDN, DCDJ, and ANT-A (models provided in the brackets). “Ex?” indicates if the method retains interpretable properties such as pure leaves, sequential decisions, and non-ensemble. “SO?” indicates if the model is self-organized (does not require a predefined structure). “EE?” indicates if the structure and weights of model are trained in an end-to-end manner.

Method	Ex?	SO?	EE?	MNIST	CIF10	CIF100	TinyIN
DDN (NiN) [23]	✗	✓	✗	-	90.32	68.35	-
DCDJ (NiN) [4]	✗	✓	✓	-	-	69.00	-
ANT-A* (n/a) [36]	✓	✓	✗	99.36	93.28	-	-
ResNet18	✗	✗	✗	98.91	94.93	75.82	63.05
DNDF [13]	✗	✗	✗	97.20	94.32	67.18	44.56
DT	✓	✗	✗	-	93.97	64.45	52.09
NBDT [38]	✓	✗	✗	-	94.82	77.09	64.23
NBDT w/o hierarchy [38]	✓	✓	✗	-	94.52	74.97	-
RDT [2]	✓	✓	✓	-	93.12	-	-
SONG (ours)	✓	✓	✓	98.81	95.62	76.26	61.99

Consequently, after restricting \mathcal{G}_x to nodes reachable with nonzero probability and removing vertices with probability zero, we obtain an acyclic graph.

Observation 4.1. *If the SONG efficiently minimizes the cost function during training, then, by Proposition 4.1, the probability of a trajectory visiting twice an arbitrary node in \mathcal{G}_x tends to zero. Consequently, we can apply Corollary 4.1 and conclude that we statistically increase accuracy when connections from each arbitrary node are binarized.*

5 Experiments

In this section, we analyze the accuracy of the SONGs trained on Letter [3], Connect4 [3], MNIST [17], CIFAR10 [14], CIFAR100 [14], and TinyImageNet [16] datasets and compare it with the state of the art methods [2, 4, 13, 23, 36, 38]. We examine how the number of nodes and steps influence the structure of graphs, the number of internal nodes used by the model, the number of backed edges, and the distance from the root to leaves. We provide a detailed comparison with SDT [8] and present sample graphs obtained for the MNIST dataset. In all experiments, we use leaves normalization and Gumbel-softmax, and we treat node regularization as a hyperparameter of the model. While this section presents only the most important findings for the sake of clarity, the experimental setup and detailed results can be found in Supplementary Materials.

SONG in deep learning setup In the first experiment, we apply SONG at the top of the backbone Convolutional Neural Network (CNN) without the final linear layer. CNN takes the input image and generates the representation, which is passed to the SONG. SONG processes the representation and returns the predictions for each class, which are then used with target labels to calculate Binary Cross-Entropy (BCE) loss. As a backbone network, we use ResNet18 for all datasets except MNIST, for which we employ a smaller network (see Supplementary Materials for details).

As presented in Table 1, our method matches or outperforms most of the recent state-of-the-art methods. On CIFAR10, SONG accuracy outperforms all baseline by almost 1 percentage point. On MNIST, it is worse than ANT [36] by around 0.5%, and on CIFAR100 and TinyImageNet, NBDT [38] achieves better results. However, both ANT and NBDT are not trained in an end-to-end manner. Moreover, NBDT requires a hierarchy provided before training, and without such a hierarchy, it obtains accuracy more than 1% lower than SONG on CIFAR100. Hence, one can expect that our model would perform better if similar auxiliary information about class hierarchy is injected into its structure.

SONG as shallow model Although SONG can be successfully used in a deep learning setup, it can also be treated as a shallow model. In this case, SONG directly processes an input sample and returns the predictions passed with target labels to BCE loss. This setup is similar to the one presented in experiments on SDTs [8]. Hence, we compare to SDT on all datasets considered in [8].

Table 2 shows that SONG obtains better results than SDT without distillation on all datasets. Moreover, on Letter and Connect4, SONG outperforms even SDT with distillation. We also observe that SONG requires fewer nodes than SDT and obtains on par results on the Connect4 dataset with 30 times fewer nodes. For Letter and MNIST, similarly good

Table 2: Comparison of SDT [8] and shallow SONG (SONG-S) on three datasets, where shallow corresponds to direct flattened inputs (no backbone network used). The accuracy of each model is reported along with the number of internal nodes specified in the parentheses. SONG-S-small contains the minimal number of nodes necessary to match the accuracy of SDT. SONG-S-large uses the same number of internal nodes as SDT.

Method	Letter	Connect4	MNIST
SDT w/o distillation [8]	78.00 (511)	78.63 (255)	94.45 (255)
SDT [8]	81.00 (511)	80.60 (255)	96.76 (255)
SONG-S-large (ours)	86.25 (511)	82.82 (255)	95.74 (255)
SONG-S-small (ours)	82.95 (64)	80.27 (8)	94.66 (64)

results can be obtained with 30 times fewer nodes. This finding is in line with [33] which shows that decision graphs require dramatically less memory while considerably improving generalization.

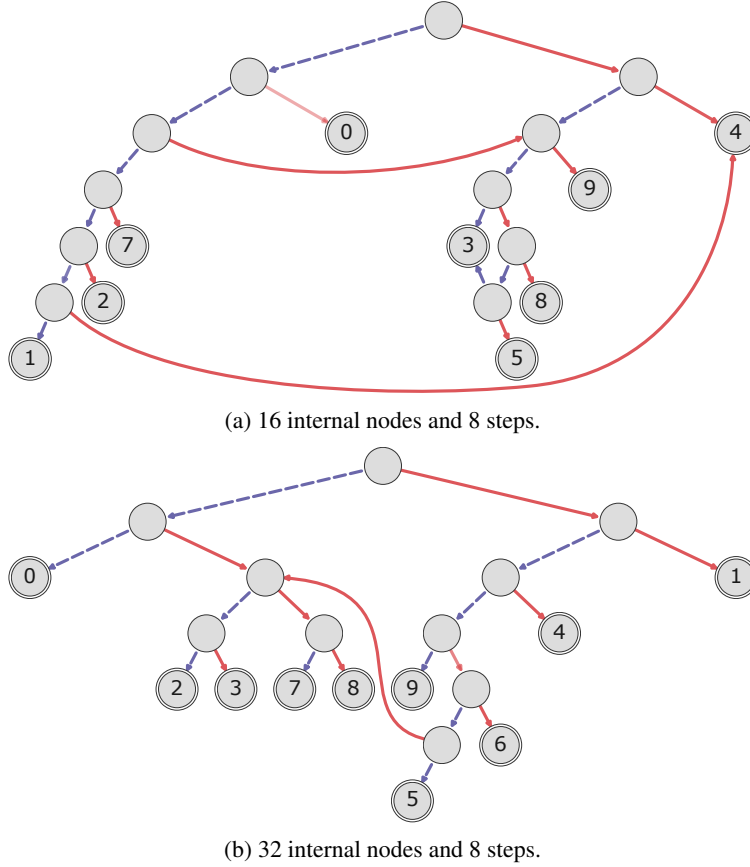


Figure 4: Examples of the graph structures obtained by training SONG on the MNIST dataset. The root is the top-most node in each graph, and the leaves are denoted by double node borders. The numbers on the leaves are the MNIST classes.

Graph structure As a fully differentiable model, SONG strengthens or weakens an edge between any pair of nodes during training to constantly optimize the graph’s structure. Consequently, it can generate any structure that uses all available nodes, or only some of them. In particular, the final structure may be a binary tree or contain back edges. Moreover, the distance from the root to leaves can vary. This variability is visualized in Figure 4, where we present two graphs obtained for MNIST using a different number of internal nodes and steps.

In Figure 5, we provide statistics on multiple SONGs generated for the MNIST dataset and observe a significant difference in SONG structure depending on the number of internal nodes and steps. First, we note that the number of internal nodes used by the model increases with the increasing number of steps N , and it does not depend on the total

number of internal nodes n . As a natural consequence, a similar trend is observed for the distance from the root to the leaves. Moreover, if the number of steps is strongly limited ($N = 4$), the model degenerates, and some of the leaves are not reachable from the root. When it comes to back edges, their number is relatively small, and they more often appear for a larger number of steps. Statistics for other datasets are in Supplementary Materials.

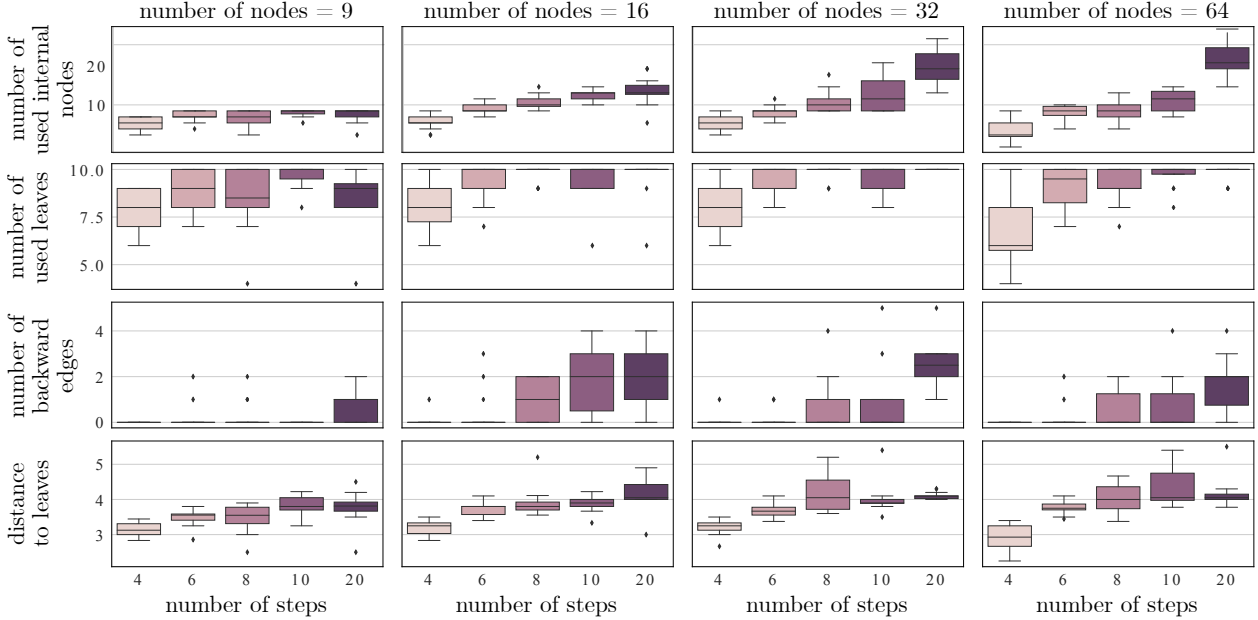


Figure 5: Node statistics calculated for SONGs trained on the MNIST dataset. For each combination of the number of internal nodes and steps, 20 graphs are trained and used to plot the distributions of 4 statistics. One can observe a significant difference in SONG structure depending on those hyperparameters.

Broader impact This work is mostly a theoretical contribution with practical elements, and as such, does not have a direct impact on society. However, our framework is a cornerstone of neural decision graphs, which sheds new light on combining modern neural networks with explainable decision models such as graphs. Hence, due to the high applicability of tree and graph decision models in many domains, our work can bring long-term benefits outside machine learning.

6 Conclusions

In this work, we introduce Self-Organizing Neural Graphs (SONGs), a new type of decision graphs applicable in any deep learning pipeline. They optimize their structure during training by strengthening or weakening graph edges using gradient descent. Thanks to the graph structure, SONG can reuse the decision nodes and obtain state-of-the-art results with a significantly smaller number of nodes than existing methods. Moreover, the introduced general paradigm based on Markov processes allows for efficient training, and SONG converges to the interpretable binary acyclic directed graphs. Hence, we believe that our work opens a plethora of research pathways towards more effective applications of decision graphs in a deep learning setup.

Appendix

A Regularizations

Our graphs require additional training regularizers, described in the paper as nodes and leaves regularizations. The nodes regularization is based on [8] and encourages each internal node to make equal use of both sets of edges \mathcal{E}^0 and \mathcal{E}^1 . For this purpose, we calculate the cross entropy between the desired average distribution 0.5, 0.5 for those two sets and the actual average distribution $\alpha_{i,s}, \beta_{i,s}$ in node v_i at step s

$$L_{nodes} = -\frac{\lambda}{2} \sum_{i=1}^n \log(\alpha_{i,s}) + \log(\beta_{i,s}),$$

where

$$\alpha_{i,s} = \frac{\sum_{x \in B} (P_x^s r)_i \cdot (\sigma_i^1(x))^\gamma}{\sum_{x \in B} (P_x^s r)_i},$$

$$\beta_{i,s} = \frac{\sum_{x \in B} (P_x^s r)_i \cdot (\sigma_i^0(x))^\gamma}{\sum_{x \in B} (P_x^s r)_i},$$

B is a batch of samples used in an iteration, $\gamma \in [1, 2]$, and $(P_x^s r)_i$ corresponds to i th coordinate of vector $(P_x^s r)$. One can observe that our nodes regularizer is calculated not per node and step. It is different from [8], where additional loss is computed once for each node. Moreover, we penalize model for making uncertain decisions ($\sigma_{i,s}(x) \approx 0.5$) using the parameter γ .

On the other hand, the leaves regularization, enforcing the summary probabilities in leaves to be close to 1, is defined as

$$L_{leaves} = -\log \left(\sum_{i=n}^{n+c} (P_x^N r)_i \right), \quad (5)$$

where n is the number of nodes (excluding root indexed with 0), c is the number of leaves (classes), and N is the number of steps.

B Experimental setup

We used the following datasets in our experiments:

- Letter (<https://archive.ics.uci.edu/ml/datasets/Letter+Recognition>),
- Connect4 (<http://archive.ics.uci.edu/ml/datasets/connect-4>),
- MNIST (published under CC BY-SA 3.0 license),
- CIFAR 10 & CIFAR 100 (published under MIT license),
- TinyImageNet (<https://www.kaggle.com/c/tiny-imagenet/data>).

Moreover, we consider two types of setups, deep (SONG) and shallow (SONG-S). In SONG, we build neural networks that contain two successive parts, CNN and a graph. For the MNIST dataset, the CNN is built from two convolution layers with 8 and 16 filters of size 5×5 , each followed by ReLU and 2×2 max pooling. Finally, a linear layer returns representation vectors of dimension 50. For other datasets (CIFAR10, CIFAR100, and TinyImageNet), we use model ResNet18 without the last linear layer. At the same time, for SONG-S, we only flatten the input sample to a one-dimensional vector.

For SONGs, we apply a similar experimental setup as in the state-of-the-art methods [38] to have comparable results. More precisely, we take the previously trained ResNet18 network, remove its last layer, and use the remaining part as a CNN part. For the MNIST data, we train the first part directly using Binary Cross Entropy (BCE) loss. For the remaining datasets, we take a model from github.com/alvinwan/neural-backed-decision-trees (published under MIT license) trained with Cross Entropy (CE) and finetune it using BCE loss. During training the SONG, weights of CNNs are frozen. Moreover, the following hyper-parameters are considered in the grid-search:

- For MNIST and CIFAR10:

- the number of nodes: 9, 16, 32, 64,
- the number of steps: 4, 6, 8, 10, 20.
- For CIFAR100:
 - the number of nodes: 99, 256, 512,
 - the number of steps: 7, 12, 20, 40.
- For TinyImagenet200:
 - the number of nodes: 512,
 - the number of steps: 20, 40.

Additionally, we consider a batch size 64 or 128 and the learning rate 0.001 for all datasets. Finally, when it comes to initialization, M^0 , M^1 , and biases in nodes are initialized from a uniform distribution on the interval $[0, 1]$, and the remaining parameters (filters in the nodes) use the Kaiming initialization.

For SONG-S, the following hyper-parameters are considered in the grid-search:

- For Letter dataset:
 - the number of nodes: 25, 32, 64, 128, 511,
 - the number of steps: 5, 10, 20, 30, 40, 50.
- For Connect4 dataset:
 - the number of nodes: 2, 8, 16, 32, 255,
 - the number of steps: 2, 5, 10.
- For MNIST dataset:
 - the number of nodes: 9, 16, 32, 64, 128, 256,
 - the number of steps: 4, 6, 8, 10, 20, 30, 40, 50.

The remaining hyper-parameters are similar to the SONG setup.

C Additional results

In this section, we provide details on the experiments conducted for SONG in a deep learning setup (see Table 3 and 4) and when treating SONG as a shallow model (see Table 5). Then, we provide the visualization of a SONG trained on MNIST where the nodes are represented by the learned filters and the “average” image passing through those nodes (see Figure 6). Moreover, we provide additional examples of the graph structures obtained by training SONG on the MNIST and CIFAR10 datasets (see Figures 7 and 8) together with the consecutive steps of the Markov process (see Figures 9, 11, 10, and 12). Finally, we show the node statistics calculated for SONGs trained on the CIFAR10 dataset (see Figure 13), and we show how the summary probabilities in leaves change during training with and without leaves regularization (see Figure 14).

Table 3: Results of SONG in a deep learning setup. One can observe that for the MNIST dataset (a), the performance increases with the increasing number of nodes and steps. In contrast to CIFAR10 (b), where the performance is relatively similar for all combinations of the parameters. It can be caused by the smaller dimension of the representation vector in MNIST (50) than in CIFAR10 (512).

(a) MNIST.					
nodes \ steps	4	6	8	10	20
9	95.66	97.29	97.25	97.95	97.56
16	97.31	97.83	98.23	98.43	98.56
32	96.82	97.74	98.35	98.65	98.62
64	96.29	98.12	98.12	98.47	98.68

(b) CIFAR10.					
nodes \ steps	4	6	8	10	20
9	94.48	94.86	94.92	94.94	94.93
16	94.88	94.95	94.86	94.87	94.89
32	94.99	94.95	94.95	94.90	94.98
64	94.90	94.87	94.88	94.94	94.93

Table 4: Results obtained for selected models from Table 3 (“base”) and their finetuned versions. We analyze two types of finetuning, either by using basis weights and finetune all the parameters of the network (“finetune”) or by taking the graph structure from the base model, reset other network parameters, and train the network from scratch (“reset”). One can observe that there is no obvious winning strategy, and they should be considered a hyperparameter. Notice also that we bold the performance reported in the main paper.

(a) MNIST.					(b) CIFAR10.				
nodes	steps	base	finetune	reset	nodes	steps	base	finetune	reset
9	10	97.95	98.43	98.67	9	10	94.94	94.98	95.26
16	8	98.23	98.81	98.66	16	6	94.95	95.09	95.47
32	8	98.35	98.61	98.81	32	6	94.95	95.12	95.62
32	10	98.65	98.52	98.71	64	10	94.94	95.03	95.41
64	20	98.68	98.63	98.72					

Table 5: SONG as a shallow model (SONG-S). One can observe that the performance increases with the increasing number of nodes and steps for all datasets. We bold the performance reported in the main paper.

(a) Letter.

steps nodes	5	10	20	30	40	50
25	52.65	63.45	62.90	63.85	67.65	68.55
32	53.65	62.65	72.90	73.30	73.20	73.55
64	57.95	74.00	78.70	79.70	82.95	82.95
128	57.00	73.85	79.60	83.05	84.45	85.75
511	48.75	72.35	81.60	82.50	84.05	86.25

(b) Connect4.

steps nodes	2	5	10
2	77.47	77.40	77.50
8	75.37	79.60	80.27
16	75.47	80.31	81.55
32	75.36	80.45	82.65
255	75.43	80.43	82.82

(c) MNIST.

steps nodes	4	6	8	10	20	30	40	50
9	87.58	88.68	88.52	88.93	89.36	90.48	90.36	90.40
16	90.74	91.73	93.06	93.09	93.42	92.97	93.39	93.37
32	88.80	91.47	93.22	93.56	94.38	93.67	93.72	93.56
64	86.35	92.77	93.33	93.41	94.66	94.29	94.86	94.55
128	90.10	93.11	93.65	94.15	94.58	94.80	94.99	94.97
255	90.05	93.11	93.80	93.88	94.28	94.75	95.43	95.74

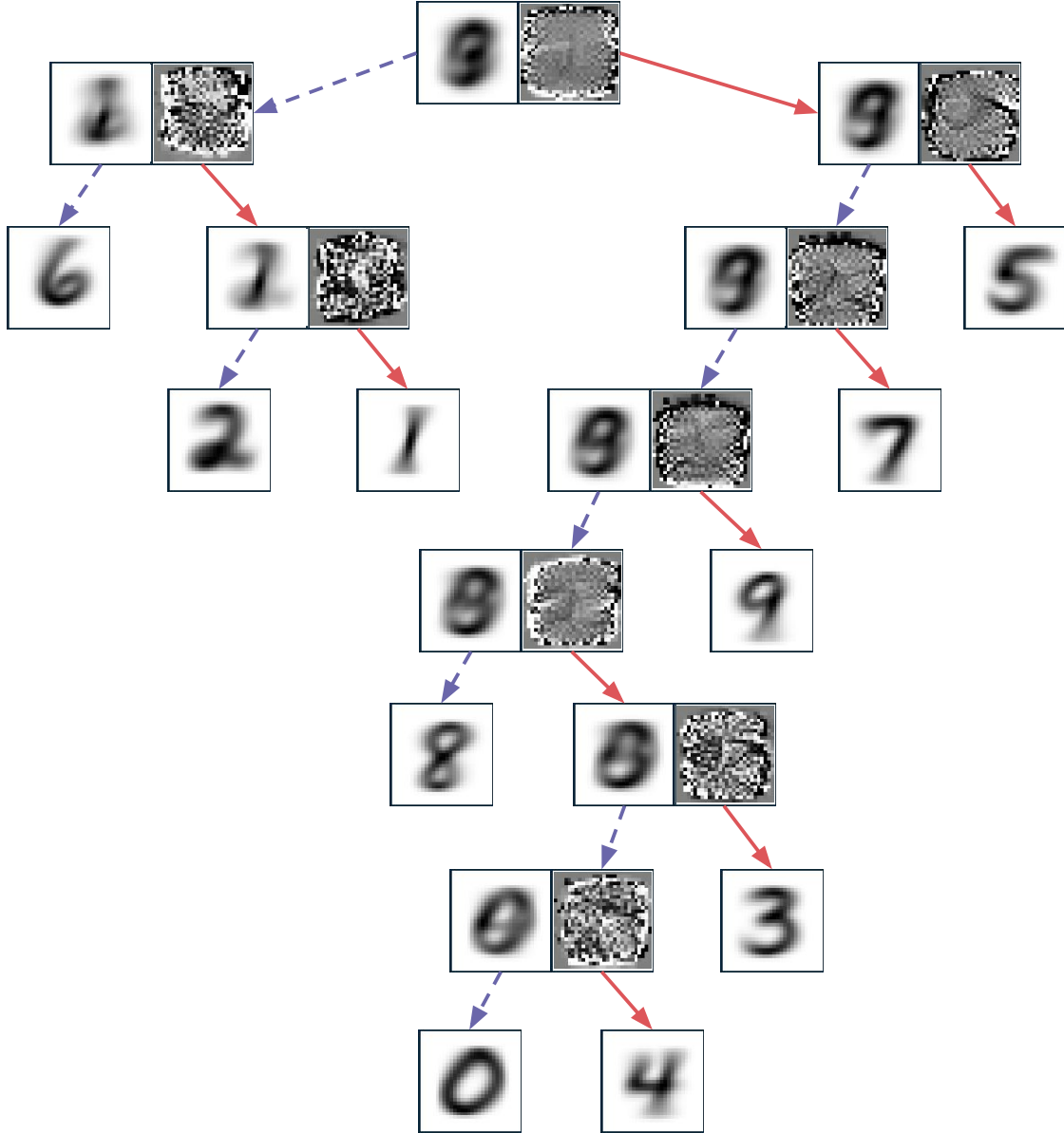


Figure 6: Visualization of a shallow SONG (SONG-S) trained on MNIST where the nodes are represented by the learned filters and the “average” image passing through those nodes (corresponding to the right and left side of each node, respectively). Notice that SONGs contain filters only in the inner nodes, as it is impossible to move out from the leaves.

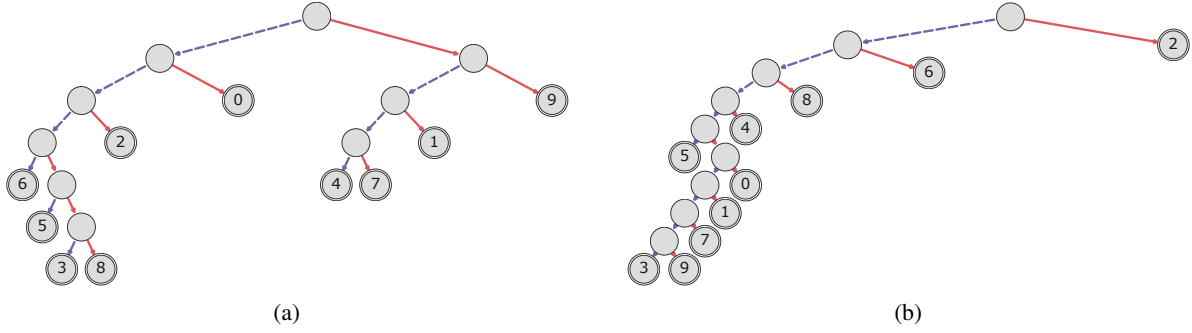


Figure 7: Examples of the graph structures obtained by training SONG on the MNIST dataset. The root is the top-most node in each graph, and the leaves are denoted by double node borders. The numbers on the leaves are the MNIST classes.

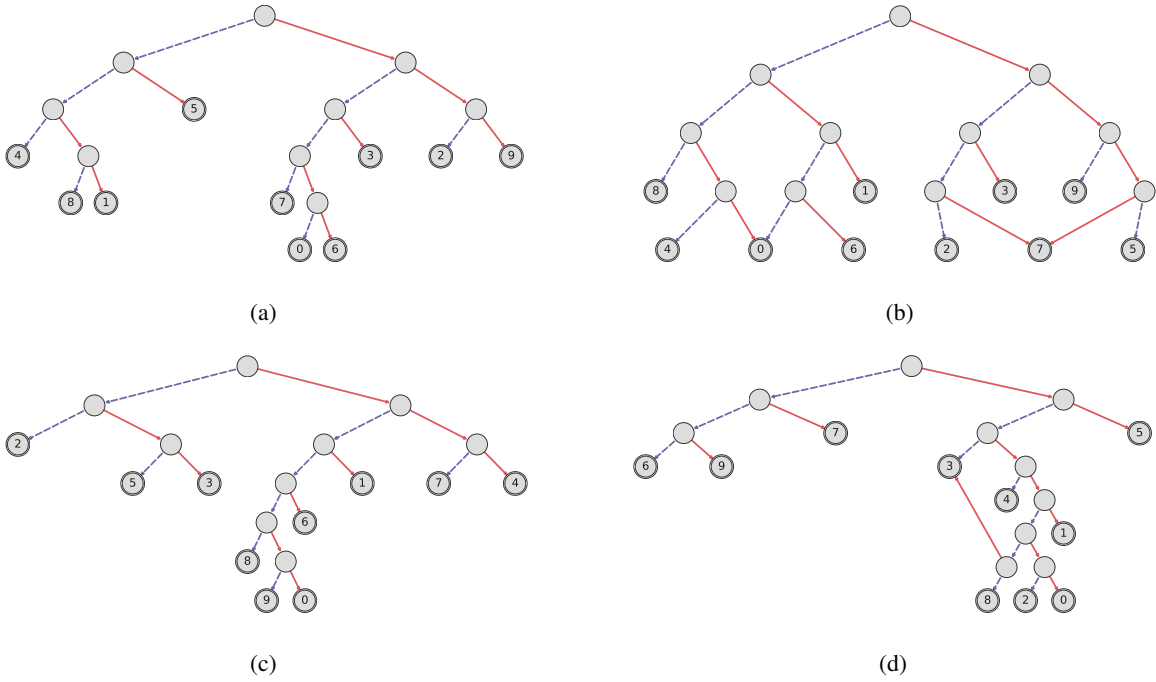


Figure 8: Examples of the graph structures obtained by training SONG on the CIFAR10 dataset. The root is the top-most node in each graph, and the leaves are denoted by double node borders. The numbers on the leaves are the CIFAR10 classes.

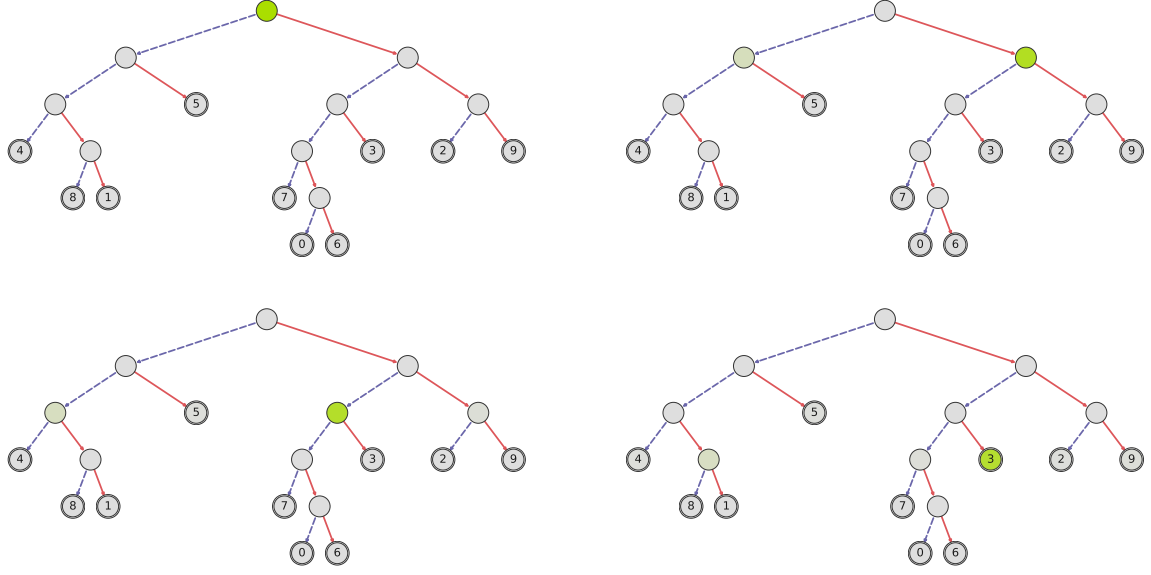


Figure 9: An input image passing through a SONG trained on CIFAR10. High saturation of the green color denotes high probability in the node. Each graph represent a consecutive step of the inference (from left to right, then top to bottom).

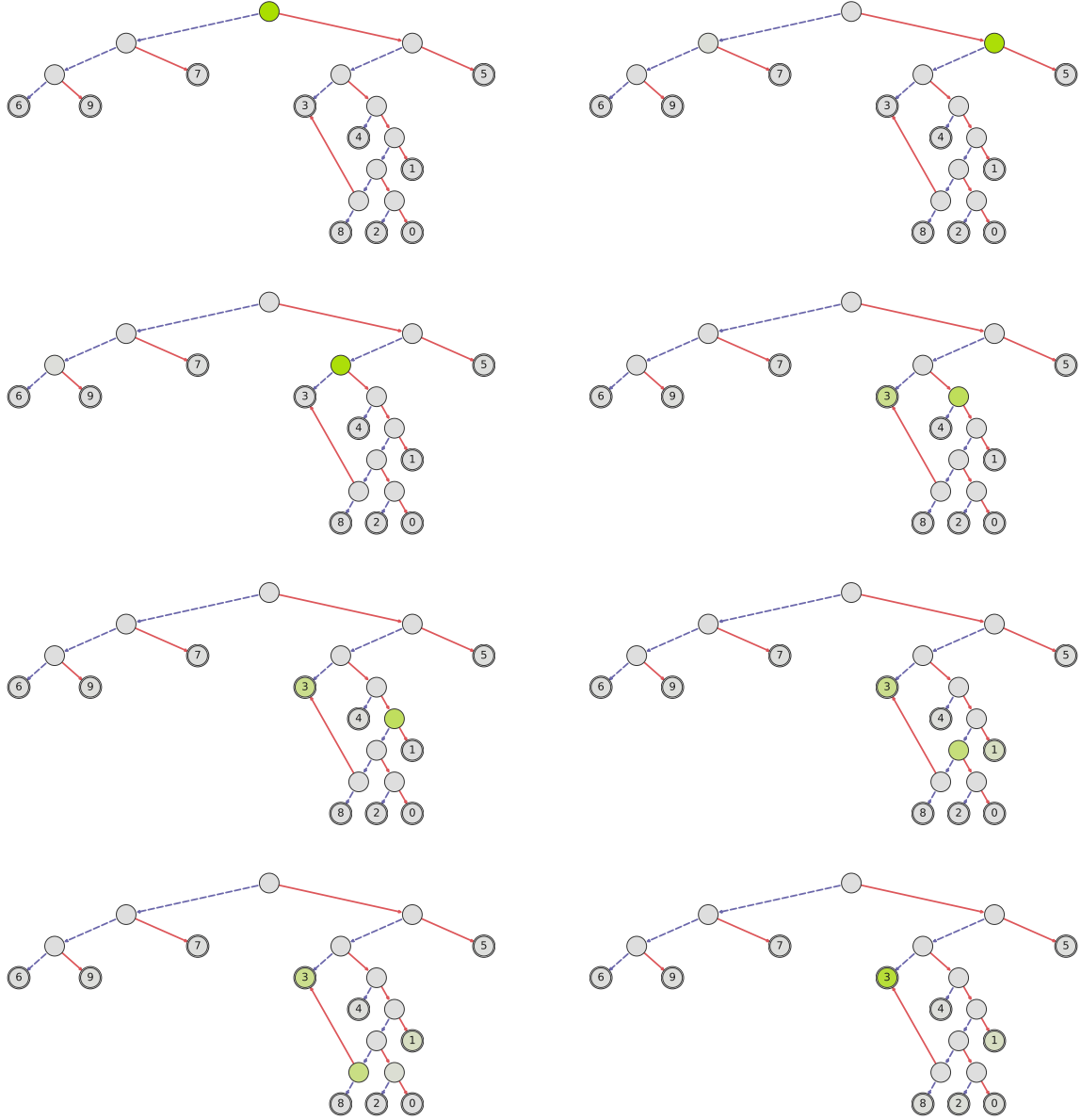


Figure 10: An input image passing through a SONG trained on CIFAR10. High saturation of the green color denotes high probability in the node. Each graph represent a consecutive step of the inference (from left to right, then top to bottom).

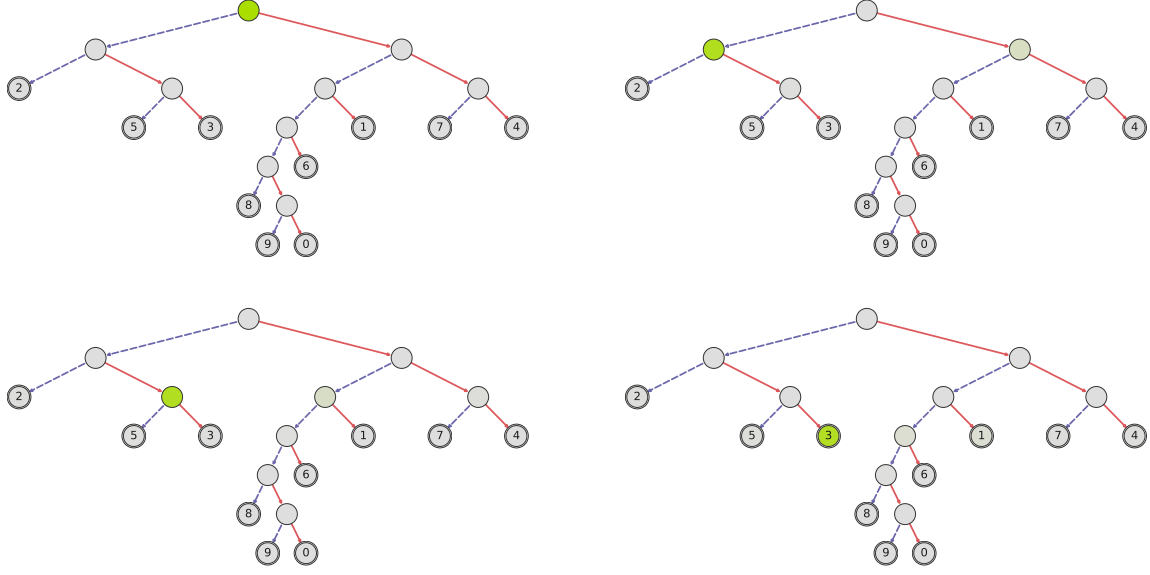


Figure 11: An input image passing through a SONG trained on CIFAR10. High saturation of the green color denotes high probability in the node. Each graph represent a consecutive step of the inference (from left to right, then top to bottom).

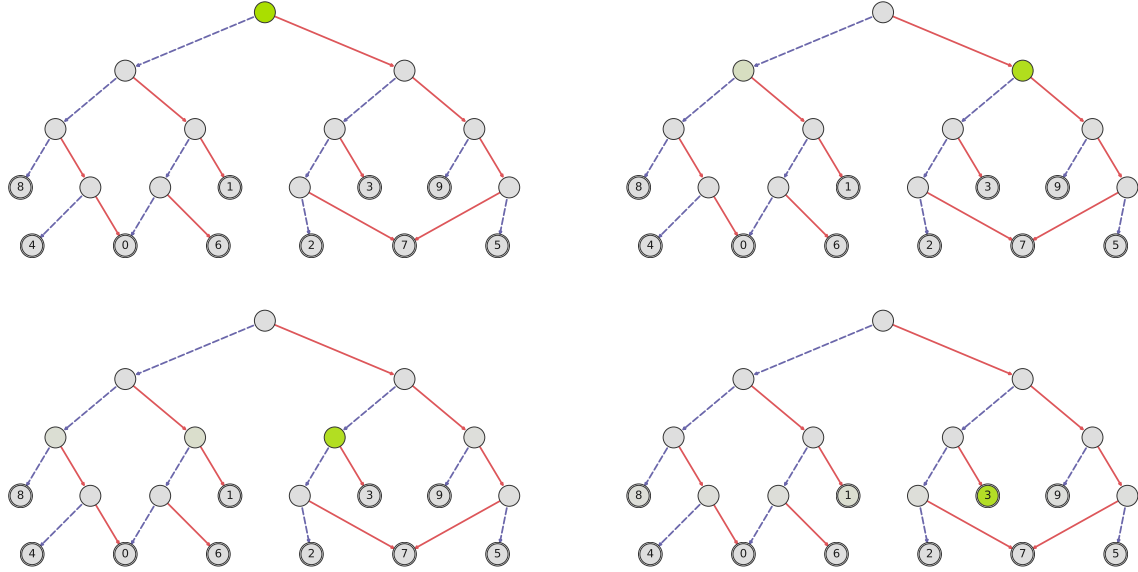


Figure 12: An input image passing through a SONG trained on CIFAR10. High saturation of the green color denotes high probability in the node. Each graph represent a consecutive step of the inference (from left to right, then top to bottom).

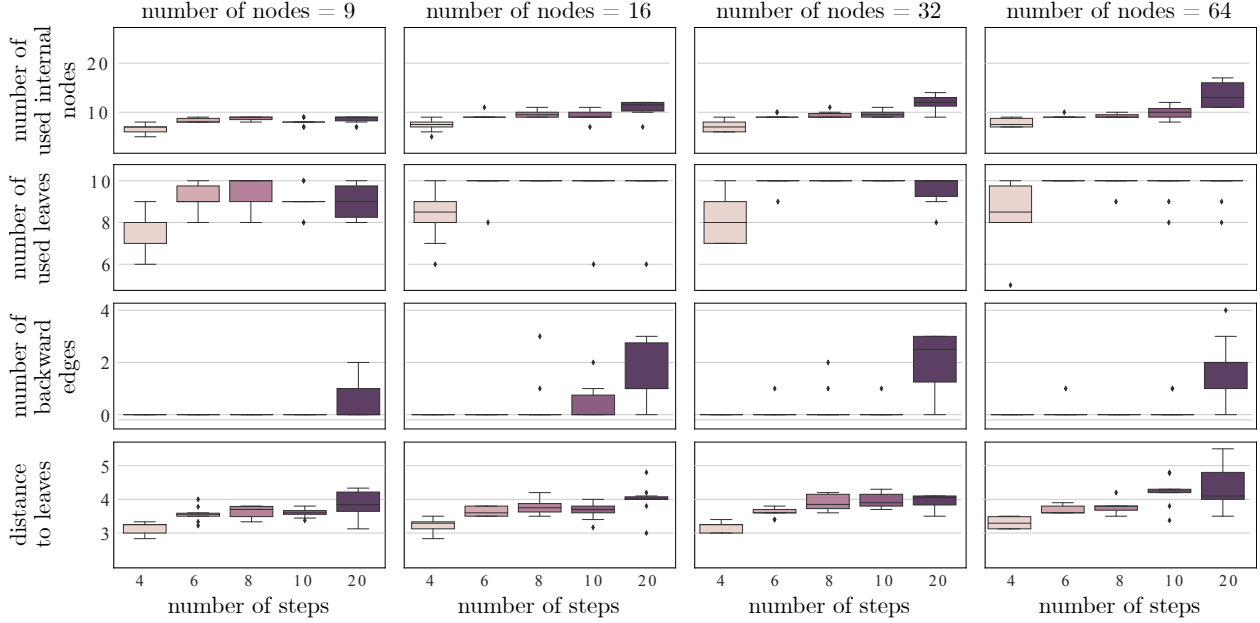


Figure 13: Node statistics calculated for SONGs trained on the CIFAR10 dataset. For each combination of the number of internal nodes and steps, 20 graphs are trained and used to plot the distributions of 4 statistics. One can observe a significant difference in SONG structure depending on those hyperparameters.

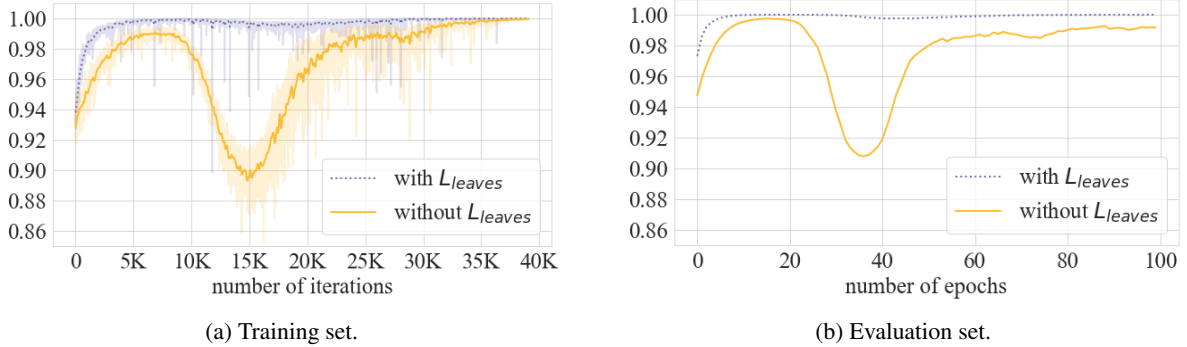


Figure 14: Summary probabilities in leaves calculated in the successive iterations of two training setups, with and without leaves regularization (5).

D Computation time and resources

We have run our experiments on Nvidia V100 32GB GPUs of our internal cluster. For deep setup, we trained 50, 50, 25, and 10 models for MNIST, CIFAR10, CIFAR100, and TinyImageNet, respectively. Each model required around 2, 2, 6, and 10 hours, respectively. For the shallow setup, we trained 60, 30, and 96 models for Letter, Connect4, and MNIST, respectively. Again, each model required around 5, 2, and 2 hours, respectively.

References

- [1] Karim Ahmed, Mohammad Haris Baig, and Lorenzo Torresani. Network of experts for large-scale image categorization. In *European Conference on Computer Vision*, pages 516–532. Springer, 2016.
- [2] Stephan Alaniz, Diego Marcos, Bernt Schiele, and Zeynep Akata. Learning decision trees recurrently through communication. In *34th IEEE Conference on Computer Vision and Pattern Recognition*. IEEE, 2021.

- [3] Arthur Asuncion and David Newman. Uci machine learning repository, 2007.
- [4] Seungryul Baek, Kwang In Kim, and Tae-Kyun Kim. Deep convolutional decision jungle for image classification. *arXiv preprint arXiv:1706.02003*, 2017.
- [5] Osbert Bastani, Carolyn Kim, and Hamsa Bastani. Interpreting blackbox models via model extraction. *arXiv preprint arXiv:1705.08504*, 2017.
- [6] Chaofan Chen, Oscar Li, Chaofan Tao, Alina Jade Barnett, Jonathan Su, and Cynthia Rudin. This looks like that: deep learning for interpretable image recognition. *arXiv preprint arXiv:1806.10574*, 2018.
- [7] Philip A. Chou. Optimal partitioning for classification and regression trees. *IEEE Computer Architecture Letters*, 13(04):340–354, 1991.
- [8] Nicholas Frosst and Geoffrey Hinton. Distilling a neural network into a soft decision tree. *arXiv preprint arXiv:1711.09784*, 2017.
- [9] Kaiming He, Xiangyu Zhang, Shaoqing Ren, and Jian Sun. Deep residual learning for image recognition. In *Proceedings of the IEEE conference on computer vision and pattern recognition*, pages 770–778, 2016.
- [10] Eric Jang, Shixiang Gu, and Ben Poole. Categorical reparameterization with gumbel-softmax. *arXiv preprint arXiv:1611.01144*, 2016.
- [11] Cem Keskin and Shahram Izadi. Splinenets: Continuous neural decision graphs. *arXiv preprint arXiv:1810.13118*, 2018.
- [12] Ron Kohavi and Chia-Hsin Li. Oblivious decision trees, graphs, and top-down pruning. In *IJCAI*, pages 1071–1079. Citeseer, 1995.
- [13] Peter Kotschieder, Madalina Fiterau, Antonio Criminisi, and Samuel Rota Buló. Deep neural decision forests. In *Proceedings of the IEEE international conference on computer vision*, pages 1467–1475, 2015.
- [14] Alex Krizhevsky, Geoffrey Hinton, et al. Learning multiple layers of features from tiny images. 2009.
- [15] Alex Krizhevsky, Ilya Sutskever, and Geoffrey E Hinton. Imagenet classification with deep convolutional neural networks. *Advances in neural information processing systems*, 25:1097–1105, 2012.
- [16] Ya Le and Xuan Yang. Tiny imagenet visual recognition challenge. *CS 231N*, 7:7, 2015.
- [17] Yann LeCun, Corinna Cortes, and CJ Burges. Mnist handwritten digit database, 2010.
- [18] Wei-Yin Loh. Classification and regression trees. *Wiley interdisciplinary reviews: data mining and knowledge discovery*, 1(1):14–23, 2011.
- [19] Manish Mehta, Rakesh Agrawal, and Jorma Rissanen. Sliq: A fast scalable classifier for data mining. In *International conference on extending database technology*, pages 18–32. Springer, 1996.
- [20] Tomáš Mikolov, Stefan Kombrink, Lukáš Burget, Jan Černocký, and Sanjeev Khudanpur. Extensions of recurrent neural network language model. In *2011 IEEE international conference on acoustics, speech and signal processing (ICASSP)*, pages 5528–5531. IEEE, 2011.
- [21] Frederic Morin and Yoshua Bengio. Hierarchical probabilistic neural network language model. In *Aistats*, volume 5, pages 246–252. Citeseer, 2005.
- [22] Ravi Teja Mullapudi, William R Mark, Noam Shazeer, and Kayvon Fatahalian. Hydranets: Specialized dynamic architectures for efficient inference. In *Proceedings of the IEEE Conference on Computer Vision and Pattern Recognition*, pages 8080–8089, 2018.
- [23] Venkatesh N Murthy, Vivek Singh, Terrence Chen, R Manmatha, and Dorin Comaniciu. Deep decision network for multi-class image classification. In *Proceedings of the IEEE conference on computer vision and pattern recognition*, pages 2240–2248, 2016.
- [24] Meike Nauta, Ron van Bree, and Christin Seifert. Neural prototype trees for interpretable fine-grained image recognition. *arXiv preprint arXiv:2012.02046*, 2020.
- [25] Arlindo L Oliveira and Alberto Sangiovanni-Vincentelli. Using the minimum description length principle to infer reduced ordered decision graphs. *Machine Learning*, 25(1):23–50, 1996.
- [26] JJ Oliver. Decision graphs - an extension of decision trees. In *Proc. 4th International Conference on Artificial Intelligence and Statistics, Miami, FL, 1993*, 1993.
- [27] Jonathan Oliver. *Decision graphs: an extension of decision trees*. Citeseer, 1992.
- [28] John C Platt, Nello Cristianini, John Shawe-Taylor, et al. Large margin dags for multiclass classification. In *nips*, volume 12, pages 547–553, 1999.

- [29] J Ross Quinlan. *C4. 5: programs for machine learning*. Elsevier, 2014.
- [30] Cynthia Rudin. Stop explaining black box machine learning models for high stakes decisions and use interpretable models instead. *Nature Machine Intelligence*, 1(5):206–215, 2019.
- [31] John Shafer, Rakesh Agrawal, and Manish Mehta. Sprint: A scalable parallel classifier for data mining. In *Vldb*, volume 96, pages 544–555. Citeseer, 1996.
- [32] Jamie Shotton, Ross Girshick, Andrew Fitzgibbon, Toby Sharp, Mat Cook, Mark Finocchio, Richard Moore, Pushmeet Kohli, Antonio Criminisi, Alex Kipman, et al. Efficient human pose estimation from single depth images. *IEEE transactions on pattern analysis and machine intelligence*, 35(12):2821–2840, 2012.
- [33] Jamie Shotton, Toby Sharp, Pushmeet Kohli, Sebastian Nowozin, John Winn, and Antonio Criminisi. Decision jungles: Compact and rich models for classification. 2016.
- [34] Alberto Suárez and James F Lutsko. Globally optimal fuzzy decision trees for classification and regression. *IEEE Transactions on Pattern Analysis and Machine Intelligence*, 21(12):1297–1311, 1999.
- [35] Hiroki Sudo, Koji Nuida, and Kana Shimizu. An efficient private evaluation of a decision graph. In *International Conference on Information Security and Cryptology*, pages 143–160. Springer, 2018.
- [36] Ryutaro Tanno, Kai Arulkumaran, Daniel Alexander, Antonio Criminisi, and Aditya Nori. Adaptive neural trees. In *International Conference on Machine Learning*, pages 6166–6175. PMLR, 2019.
- [37] Andreas Veit and Serge Belongie. Convolutional networks with adaptive inference graphs. In *Proceedings of the European Conference on Computer Vision (ECCV)*, pages 3–18, 2018.
- [38] Alvin Wan, Lisa Dunlap, Daniel Ho, Jihan Yin, Scott Lee, Henry Jin, Suzanne Petryk, Sarah Adel Bargal, and Joseph E Gonzalez. Nbd: neural-backed decision trees. *ICLR 2021*, 2020.
- [39] Quanshi Zhang, Yu Yang, Haotian Ma, and Ying Nian Wu. Interpreting cnns via decision trees. In *Proceedings of the IEEE/CVF Conference on Computer Vision and Pattern Recognition*, pages 6261–6270, 2019.